Short Note

Journal of Labelled Compounds and Radiopharmaceuticals

Received 19 March 2014, Revised 28 May 2014, Accepted 30 June 2014 Published online in Wiley Online Library

(wileyonlinelibrary.com) DOI: 10.1002/jlcr.3220

Toward hyperpolarized molecular imaging of HIV: synthesis and longitudinal relaxation properties of ^{15}N-Azidothymidine

Roman V. Shchepin[a]* and Eduard Y. Chekmenev[a,b,c]*

Previously unreported ^{15}N labeled Azidothymidine (AZT) was prepared as an equimolar mixture of two isotopomers: 1-^{15}N-AZT and 3-^{15}N-AZT. Polarization decay of ^{15}N NMR signal was studied in high (9.4 T) and low (~50 mT) magnetic fields. ^{15}N T_1 values were 45 ± 5 s (1-^{15}N-AZT) and 37 ± 2 s (3-^{15}N-AZT) at 9.4 T, and 140 ± 16 s (3-^{15}N-AZT) at 50 mT. ^{15}N-AZT can be potentially ^{15}N hyperpolarized by several methods. These sufficiently long ^{15}N-AZT T_1 values potentially enable hyperpolarized *in vivo* imaging of ^{15}N-AZT, because of the known favorable efficient (i.e., of the time scale shorter than the longest reported here ^{15}N T_1) kinetics of uptake of injected AZT. Therefore, 3-^{15}N-AZT can be potentially used for HIV molecular imaging using hyperpolarized magnetic resonance imaging.

Keywords: hyperpolarization; contrast agent; azidothymidine; 15N; MRI; AZT; HIV; AIDS

Introduction

There are approximately 35 million people with HIV worldwide as of 2012[1] with 1.2 million of them living in the USA. This disease has no cure or vaccine, and HIV/AIDS is managed by administration of one or more antiretroviral drugs. The course of management and the disease progression in monitored by blood tests to measure the viral and CD4 cell counts in blood. However, these tests repeated every 3–6 months do not directly report on the viral load in other tissues such as lymph nodes, spleen, or brain. Furthermore, when patient's viral count is reduced below the detection limit (<50 copies/mL),[2] there is no gauge to measure the response to treatment and identify more effective choice of treatment until the disease manifests again as the elevated level of HIV virus in blood. Information about disease progression beyond blood tests is critically important for disease management, progression, response to treatment, and development of new drugs and vaccines.

Molecular imaging significantly improved patients' management in cancer, where the elevated metabolism of cancer cells can be imaged with radioactive and hyperpolarized (HP)[3] contrast agents. HIV/AIDS does not have clear metabolic signatures that can be interrogated by F18-fluorodeoxyglucose positron emission tomography for distinguishing the disease progression.[4] Therefore, other molecular imaging probes are required to report on HIV progression by targeting HIV/AIDS signatures. Multiple approaches of molecular imaging beyond metabolite (e.g., glucose, glutamine, and choline) imaging are feasible including receptor imaging via targeted positron emission tomography[5] and HP molecular magnetic resonance imaging (MRI)[6] probes. An alternative approach is to image the drug molecule itself. While this can be challenging if not impossible from the perspective of radioactive isotope incorporation due to sophisticated chemistry and short life time of biomedically useful nuclei, emerging HP MRI offers clear benefit of dividing the challenging task of contrast agent preparation in two parts: (i) chemical synthesis of the molecule with isotopically enriched nuclei biochemically identical to the drug, for example, incorporation of ^{13}C or ^{15}N and (ii) contrast agent preparation step, for example, hyperpolarization that makes the enriched molecule activated and useful for molecular imaging. Despite MRI sensitivity gains by orders of magnitude achieved by hyperpolarization process,[7,8] the ultimate limitation of HP approaches is still the detection sensitivity,[9] which requires a human dose of hundreds of milligrams of imaging contrast agent. Therefore, the use of HP molecular imaging using isotopically enriched treatment drugs is limited to those injected in relatively large quantities.

Azidothymidine (AZT) or Zidovudine is a Food and Drug Administration approved nucleoside analog reverse transcriptase inhibitor, a type of antiretroviral medication.[10] It is used for the treatment of HIV/AIDS as well as for prevention of the infection transmission such as mother to child during the period of birth.[11] It has been shown that AZT acts by competing with 3′-deoxythymidine-5′-triphosphate, for incorporation into DNA by HIV-reverse transcriptase.[12] Incorporation of AZT monophosphate into DNA by HIV-reverse transcriptase results in chain termination. Because of its potency as well as the fact that AZT presently available as a 'generic drug', it is used in many combined formulations including Combivir and Trizivir.[13] Furthermore, AZT can be administered in doses of ~1 g and therefore is a suitable candidate for HP imaging probe, which can potentially allow for imaging of injected HP

[a]*Department of Radiology, Vanderbilt University Institute of Imaging Science (VUIIS), Nashville, TN 37232, USA*

[b]*Department of Biomedical Engineering, Vanderbilt University, Nashville, TN 37235, USA*

[c]*Department of Biochemistry, Vanderbilt University, Nashville, TN 37205, USA*

**Correspondence to: Roman V. Shchepin and Eduard Y. Chekmenev, Department of Radiology, Vanderbilt University Institute of Imaging Science (VUIIS), Nashville, TN 37232, USA.*
E-mail: roman.shchepin@vanderbilt.edu; eduard.chekmenev@vanderbilt.edu

contrast agent that has good affinity to HIV's reverse transcriptase[12] and cell membrane permeability enabled by the azide moiety.

Azide group (N_3) in the AZT molecular structure can be labeled with ^{15}N isotope, which can be used for hyperpolarization and hyperpolarization storage during agent administration and uptake, Figure 1. Several hyperpolarization approaches can be used for ^{15}N-AZT hyperpolarization. For instance, dynamic nuclear polarization,[14] presently the most widespread hyperpolarization technique, can be potentially employed similarly to hyperpolarization of other ^{15}N compounds including choline.[15] Additionally, Signal Amplification by Reversible Exchange[16,17] method can provide a good opportunity for ^{15}N-AZT hyperpolarization, because the unsaturated nitrogens in azide moiety can be potentially employed for reversible exchange. Furthermore, parahydrogen induced polarization (PHIP)[18,19] can be also potentially applied, because AZT structure allows for the incorporation of an unsaturated C=C bond in the PHIP molecular hyperpolarization precursor. Similar in complexity, ^{15}N compounds have been developed[20] and ^{15}N HP[21] by PHIP. Regardless of hyperpolarization approach to be applied, ^{15}N isotopic enrichment of AZT is required, which was successfully demonstrated here. Moreover, the delivery of HP contrast agent, Figure 1, requires sufficiently long lifetime of produced contrast agent. The ^{15}N T_1 relaxation properties of the produced ^{15}N-AZT that were investigated here provide critical information for future hyperpolarization and imaging efforts, Figure 1.

Experimental methods

General

All solvents were purchased from common vendors and were used as received. New AZT isotopomer was characterized by ^{1}H, ^{13}C, ^{15}N NMR (Bruker 400 MHz), and high-resolution mass spectrometry (HR-MS). HR mass spectra were recorded in negative mode using a Synapt hybrid quadrupole/oa-TOF mass spectrometer (Waters Corp., Milford, MA) equipped with a dual chemical ionization/electrospray (ESCI) source. A post-acquisition gain correction was applied using a solution of 3-[(3-holamidopropyl)dimethylammonio]-1-propanesulfonate (CHAPS, FW 614.88) as the lock mass spray.

^{15}N-AZT preparation

^{15}N-AZT was prepared similar to Czernecki procedure,[22] where sodium azide-1-^{15}N (Sigma-Aldrich, 609374) was used in place of natural isotopic abundance lithium azide. No recrystallization of final product was performed because of the small synthetic scale.

2,3′-Anhydro-5′-O-(4-methoxybenzoyl)thymidine [22]

Thymidine (3.63 g, 15 mmol) and Ph_3P (5.9 g, 22.5 mmol, 1.5 equiv.) are dissolved in dimethylformamide (DMF) (30 mL), and the solution cooled to 15 °C on a water bath. To this stirred mixture, a solution of diisopropyl azodicarboxylate (4.4 mL, 22.5 mmol, 1.5 equiv.) in DMF (7 mL) and 4-methoxybenzoic acid (3.42 g, 22.5 mmol, 1.5 equiv.) is added drop-by-drop, and stirring is continued at room temperature (r. t.) for 15 min. The same quantity of Ph_3P and diisopropyl azodicarboxylate is then added. After 30 min. at r. t., the mixture is poured into Et_2O (370 mL), and the resulting suspension is chilled for 2 h. The white crystalline precipitate is isolated by suction and washed with Et_2O; yield: 4 g (74% yield).

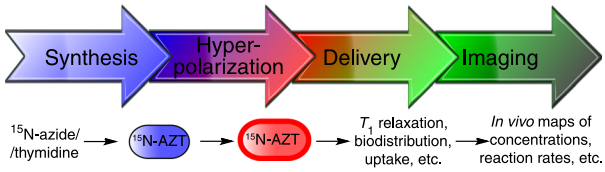

Figure 1. Overall approach of development of hyperpolarized contrast agents for molecular imaging.

3′-Azido-3′-deoxy-5′-O-(4-methoxybenzoyl)thymidine

2,3′-Anhydro-5′-*O*-(4-methoxybenzoyl)thymidine (1.00 g, 2.8 mmol) and sodium azide-1-^{15}N (273 mg, 4.2 mmol, 1.5 equiv.) are suspended in DMF (10 mL), and the mixture is heated on an oil bath at 125 °C for 5 h. The orange homogeneous mixture is poured in H_2O (25 mL) containing 5% aq HCl (2.0 mL, 1 equiv.), EtOAc (15 mL) is added. The aqueous layer is extracted with EtOAc (2 × 10 mL), and the organic extract is washed with H_2O (7 mL), then with brine (7 mL). After drying (Na_2SO_4), the solvent is evaporated *in vacuo* to give 3′-azido-3′-deoxy-5′-*O*-(4-methoxybenzoyl)thymidine-1-^{15}N as a foamy solid; yield: 1 g (90% nominal yield). Crude 3′-azido-3′-deoxythymidine: 3′-azido-3′-deoxy-5′-*O*-(4-methoxybenzoyl)thymidine-1-^{15}N (1.0 g, 2.5 mmol) is suspended in dry MeOH (10 mL), 1 M NaOMe in MeOH (2.9 mL, 1.15 equiv.) is added, and the mixture is stirred at r.t. overnight (12 h). H_2O (15 mL) is added, and MeOH is evaporated. The aqueous solution is extracted with Et_2O (2 × 10 mL), then Amberlite IRN-77 (H^+ form, 1 g) is added, and the mixture is stirred slowly at r.t. for 15 min. The resin is filtered, washed well with H_2O, and the filtrate is concentrated *in vacuo* to give a white glassy solid: 3′-azido-3′-deoxythymidine-1-^{15}N (^{15}N-AZT) yield: 0.270 g (40%).

^{1}H (D_2O, 400 MHz) δ: 7.50 (d, 1H, *J*(HH) = 1.2 Hz), 6.05 (pseudo-t, 1H, *J*(HH) = 6.5 Hz), 4.22 (dd, 1H, *J*(HH) = 6.4 Hz, and *J*(HH) = 12.0 Hz), 3.87 (m, 1H), 3.73 and 3.63 (dAB, 2 H, *J*(HH)gem = 12.6 Hz, *J*(HH)vic = 4.6 Hz), 2.35 (superposition of normal triplet (3-^{15}N-AZT), 1H, *J*(HH) = 6.5 Hz and doublet of triplets (1-^{15}N-AZT), 1H, *J*(HH) = 6.5 Hz and *J*(H-^{15}N) = 2.6 Hz) 1.74 (d, 3H, *J*(HH) = 1.1); $^{13}C\{^{1}H\}$ (D_2O The spectrum was referenced externally to chloroform-*d* (77 ppm), 100 MHz) δ: 166.7, 151.7, 137.2, 111.1, 84.7, 83.9, 60.7, 59.6, 35.8, 11.4; $^{15}N\{^{1}H\}$ (D_2O, The spectrum was referenced externally to ^{15}N-urea, 76 ppm) 214.9, 75.9 (*J*(H-^{15}N) = 2.6 Hz). HR-MS calculated for (M-1): 267.0865; found: 267.0864 (0.4 ppm).

^{15}N T_1 NMR Measurements at 9.4 T. Nuclear magnetic resonance sample was prepared by dissolving ^{15}N-AZT in 0.50 mL of D_2O at the maximum concentration (~20 mg/mL at 25 °C). T_1 inversion recovery pulse sequence (as supplied by Bruker Biospin) was used to measure ^{15}N T_1 at 9.4 T. ^{15}N NMR signals of the two ^{15}N sites were integrated (using the same scale for all the spectra) in resulting set of 1D spectra with varied inversion recovery delay, Figure 2b and 2c. Mono-experiential decay fitting model ($y = C \cdot \exp(-x/T_1) + y_0$) was used for each ^{15}N resonance time series data.

^{15}N T_1 NMR Measurements at 50 mT. The aforementioned NMR sample was used in the field-cycling ^{15}N T_1 experiment, where the NMR sample was first polarized inside 400 MHz NMR spectrometer for ~5 min, which significantly exceeds T_1 at 9.4 T. Then, the sample was lifted from 9.4 T magnetic field, and it was exposed to the low fringe field ($B_0 = 50 \pm 5$ mT) of the main NMR magnet. Finally, the sample was quickly placed back inside the 400 MHz NMR spectrometer, and a single scan ^{15}N NMR spectrum was collected without any additional delay. This cycling operation was repeated with variable low-field sample exposure. Integral values of 3-^{15}N signal were plotted versus time spent in the low magnetic field. Mono-experiential decay fitting model ($y = C \cdot \exp(-x/T_1) + y_0$) was used for 3-$^{15}N$ resonance time series data. All fitting and error analyses were performed using Microcal Origin software.

Results and discussion

In Czernecki procedure[22] (Figure 2a), thymidine is protected with *p*-methoxybenzyl ether with inversion of 3′-OH center. Lithium azide with natural isotopic abundance was replaced by sodium 1-^{15}N-azide substitution step (Figure **2**a, II). Because of the double inversion overall stereochemistry of AZT is the same as that of thymidine. Because symmetric azide anion was labeled only on one of two ends, the reaction sequence produced equimolar mixture of two isotopomers **1-^{15}N-AZT** and **3-^{15}N-AZT** (Figure **2**a) in excellent isotopic purity and satisfactory overall purity (Figures S1–S4).

Journal of Labelled Compounds and Radiopharmaceuticals

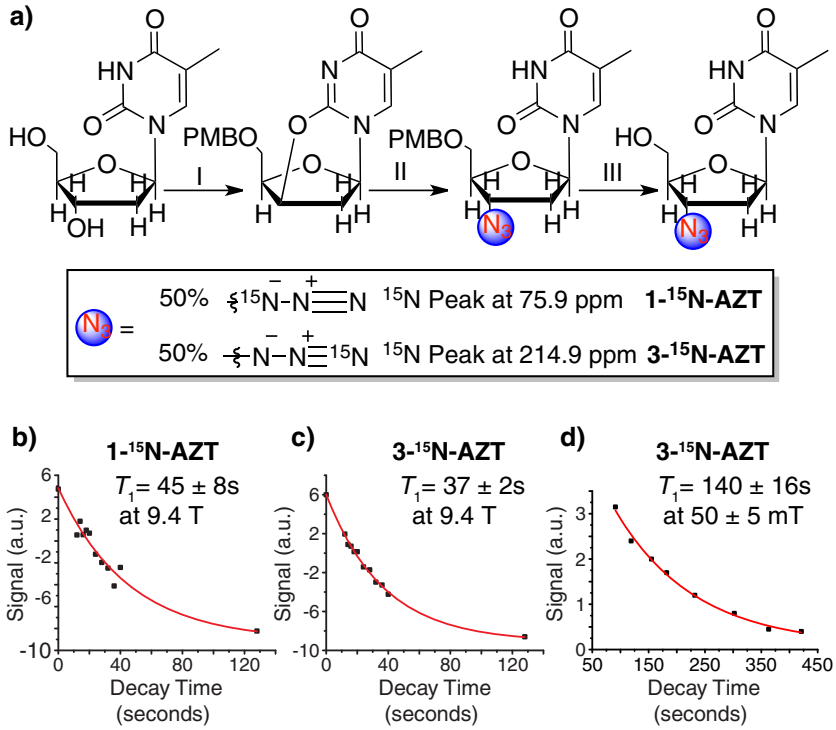

Figure 2. (a) ^{15}N-AZT preparation: (I) DIAD (1.5 eq)/Ph_3P (1.5 eq), 4-$MeOC_6H_4CO_2H$ (1.5 eq) DMF, DIAD (1.5 eq)/Ph_3P (1.5 eq); (II) Sodium 1-^{15}N-azide, DMF; (III) MeONa / MeOH. (b) Polarization recovery of ^{15}N resonance at 75.9 ppm (1-^{15}N-AZT) at 9.4 T. (c) Polarization recovery of ^{15}N resonance at 214.9 ppm (3-^{15}NAZT) at 9.4 T. (d) Polarization decay of ^{15}N resonance at 214.9 ppm measured by sample exposure to 50 ± 5 mT magnetic field.

Preparation of ^{15}N-AZT enabled measurement of the polarization T_1 decay of two ^{15}N sites, which is a critical parameter determining the feasibility of HP imaging and *in vivo* applications, Figure 1. ^{15}N T_1 values were 45 ± 5 s for 1-^{15}N-AZT (^{15}N peak at 75.9 ppm) and 37 ± 2 s for 3-^{15}N-AZT (^{15}N peak at 214.9 ppm), respectively, at 9.4 T, Figure 2. ^{15}N T_1 values were 140 ± 16 s for 3-^{15}N-AZT at 50 mT. ^{15}N T_1 values measured at 9.4 T (35–50 s) were significantly shorter than that at 50 mT, Figure 2. This difference is likely explained by differential contribution of ^{15}N chemical shift anisotropy (CSA) at high and low magnetic fields, because ^{15}N CSA over 700 ppm (corresponding to ~30 kHz at this magnetic field) is not uncommon.[23] When the magnetic field is reduced to 50 mT, the CSA contribution is negligible, because CSA scales linearly with magnetic field, it is reduced by ~200-fold in units of Hertz. ^{15}N T_1 decay of 1-^{15}N-AZT in the low magnetic field was very rapid, and T_1 was very challenging to quantify, which is related to the relatively slow speed of NMR sample lifting from the NMR spectrometer. A possible explanation of significantly shorter low-field 1-^{15}N-AZT T_1 is an accelerated relaxation due to the neighboring protons of the five-membered ring.

While the high-field ^{15}N T_1 values may be sufficient for the preparation of HP AZT and its ^{15}N *in vivo* imaging[24], low-field detection would be clearly advantageous, because of the nearly threefold increase in T_1. It should be noted that low-field HP imaging can be more sensitive than high-field HP imaging in general,[25,26] and low-field MRI of HP AZT uptake would be clearly attractive. Furthermore, the detection sensitivity of HP ^{15}N sites can be further amplified by indirect proton detection of HP contrast agents.[27,28] While the latter is challenging (but certainly feasible) in high-field MRI applications, because water protons generate large background signal,[29,30] the water proton background can be attenuated by orders of magnitude in low-field MRI <0.1 T.[26]

The previous work in cellular model[31] demonstrated rapid uptake of AZT by human cell with nearly linear intracellular AZT uptake during first 20 s with peak plateau achieved in less than 100 s, which is certainly within $1 \times T_1$ of ^{15}N spin label that is potentially amenable to hyperpolarization. We point out that HP compounds are useful for imaging within $(1-3) \times T_1$ period after their *in vivo* administration.[9] Moreover, this uptake kinetics holds true even at high extracellular AZT concentration up to 50 mM.[31] The latter is well below plasma AZT concentration of treated patients with subgram dose. While it remains to be seen (i) if sufficient *in vivo* signal can be detected with HP AZT and (ii) if the *in vivo* viral uptake will be sufficient to generate imaging contrast, the kinetics of hyperpolarization decay (this work) and cellular uptake[31] are certainly promising to support such future studies.

Conclusions

Synthetic preparation of ^{15}N analog of antiviral drug AZT has been demonstrated. While both ^{15}N-AZT isotopomers have sufficiently long high-field ^{15}N T_1 (~35–50 s) for potential use in future pre-clinical and clinical studies, 3-^{15}N-AZT is particularly promising, because it has an ultra-long T_1 in excess of 2 min at low magnetic field. This makes 3-^{15}N-AZT a promising candidate for future HP imaging efforts for molecular imaging of HIV/AIDS.

Acknowledgements

We gratefully acknowledge the financial support from NIH/NCI 5R00 CA134749-03, 3R00CA134749-02S1 and Department of Defense CDMRP Era of Hope Award W81XWH-12-1-0159/BC112431.

Conflict of Interest

The authors did not report any conflict of interest.

References

[1] UNAIDS.org. **2013**, p. Fact Sheet. http://www.unaids.org/en/resources/campaigns/globalreport2013/factsheet/ [6 Feb. 2014].
[2] S. M. Hammer, J. J. Eron, P. Reiss, et al., *JAMA* **2008**, *300*, 555.
[3] S. J. Nelson, J. Kurhanewicz, D. B. Vigneron, P. E. Z. Larson, A. L. Harzstark, M. Ferrone, M. van Criekinge, J. W. Chang, R. Bok, I. Park, G. Reed, L. Carvajal, E. J. Small, P. Munster, V. K. Weinberg, J. H. Ardenkjaer-Larsen, A. P. Chen, R. E. Hurd, L. I. Odegardstuen, F. J. Robb, J. Tropp, J. A. Murray, *Sci. Transl. Med.* **2013**, *5*, 1.
[4] D. Brust, M. Polis, R. Davey, B. Hahn, S. Bacharach, M. Whatley, A. S. Fauci, J. A. Carrasquillo, *Aids* **2006**, *20*, 495.
[5] D. Tang, E. T. McKinley, M. R. Hight, M. I. Uddin, J. M. Harp, A. Fu, M. L. Nickels, J. R. Buck, H. C. Manning, *J. Med. Chem.* **2013**, *56*, 3429.
[6] P. Bhattacharya, E. Y. Chekmenev, W. F. Reynolds, S. Wagner, N. Zacharias, H. R. Chan, R. Bünger, B. D. Ross, *NMR Biomed.* **2011**, *24*, 1023.
[7] K. Golman, O. Axelsson, H. Johannesson, S. Mansson, C. Olofsson, J. S. Petersson, *Magn. Reson. Med.* **2001**, *46*, 1.
[8] J. H. Ardenkjaer-Larsen, B. Fridlund, A. Gram, G. Hansson, L. Hansson, M. H. Lerche, R. Servin, M. Thaning, K. Golman, *Proc. Natl. Acad. Sci. U. S. A.* **2003**, *100*, 10158.
[9] J. Kurhanewicz, D. Vigneron, K. Brindle, E. Chekmenev, A. Comment, C. Cunningham, R. DeBerardinis, G. Green, M. Leach, S. Rajan, R. Rizi, B. Ross, W. S. Warren, C. Malloy, *Neoplasia* **2011**, *13*, 81.
[10] K. Wright, *Nature* **1986**, *323*, 283.
[11] B. G. Brenner, M. A. Wainberg, *Ann. N. Y. Acad. Sci.* **2000**, *918*, 9.
[12] P. A. Furman, J. A. Fyfe, M. H. St Clair, K. Weinhold, J. L. Rideout, G. A. Freeman, S. N. Lehrman, D. P. Bolognesi, S. Broder, H. Mitsuya, et al., *Proc. Natl. Acad. Sci. U. S. A.* **1986**, *83*, 8333.
[13] G. D'Andrea, F. Brisdelli, A. Bozzi, *Curr. Clin. Pharmacol.* **2008**, *3*, 20.
[14] A. Abragam, M. Goldman, *Rep. Prog. Phys.* **1978**, *41*, 395.
[15] C. Gabellieri, S. Reynolds, A. Lavie, G. S. Payne, M. O. Leach, T. R. Eykyn, *J. Am. Chem. Soc.* **2008**, *130*, 4598.
[16] R. W. Adams, J. A. Aguilar, K. D. Atkinson, M. J. Cowley, P. I. P. Elliott, S. B. Duckett, G. G. R. Green, I. G. Khazal, J. Lopez-Serrano, D. C. Williamson, *Science* **2009**, *323*, 1708.
[17] K. D. Atkinson, M. J. Cowley, P. I. P. Elliott, S. B. Duckett, G. G. R. Green, J. Lopez-Serrano, A. C. Whitwood, *J. Am. Chem. Soc.* **2009**, *131*, 13362.
[18] C. R. Bowers, D. P. Weitekamp, *Phys. Rev. Lett.* **1986**, *57*, 2645.
[19] T. C. Eisenschmid, R. U. Kirss, P. P. Deutsch, S. I. Hommeltoft, R. Eisenberg, J. Bargon, R. G. Lawler, A. L. Balch, *J. Am. Chem. Soc.* **1987**, *109*, 8089.
[20] R. V. Shchepin, E. Y. Chekmenev, *J. Labelled Comp. Radiopharm.* **2013**, *56*, 655.
[21] F. Reineri, A. Viale, S. Ellena, D. Alberti, T. Boi, G. B. Giovenzana, R. Gobetto, S. S. D. Premkumar, S. Aime, *J. Am. Chem. Soc.* **2012**, *134*, 11146.
[22] S. Czernecki, J.-M. Valery, *Synthesis* **1991**, *1991*, 239.
[23] R. L. Koder, J. D. Walsh, M. S. Pometun, P. L. Dutton, R. J. Wittebort, A. F. Miller, *J. Am. Chem. Soc.* **2006**, *128*, 15200.
[24] C. Cudalbu, A. Comment, F. Kurdzesau, R. B. van Heeswijk, K. Uffmann, S. Jannin, V. Denisov, D. Kirik, R. Gruetter, *Phys. Chem. Chem. Phys.* **2010**, *12*, 5818.
[25] A. M. Coffey, R. V. Shchepin, K. Wilkens, K. W. Waddell, E. Y. Chekmenev, *J. Magn. Reson.* **2012**, *220*, 94.
[26] A. M. Coffey, M. L. Truong, E. Y. Chekmenev, *J. Magn. Reson.* **2013**, *237*, 169.
[27] E. Y. Chekmenev, V. A. Norton, D. P. Weitekamp, P. Bhattacharya, *J. Am. Chem. Soc.* **2009**, *131*, 3164.
[28] R. Sarkar, A. Comment, P. R. Vasos, S. Jannin, R. Gruetter, G. Bodenhausen, H. Hall, D. Kirik, V. P. Denisov, *J. Am. Chem. Soc.* **2009**, *131*, 16014.
[29] M. Mishkovsky, A. Comment, R. Gruetter, *J. Cereb. Blood Flow Metab.* **2012**, *32*, 2108.
[30] M. L. Truong, A. M. Coffey, R. V. Shchepin, K. W. Waddell, E. Y. Chekmenev, *Contrast Media Mol. Imaging* **2013**, DOI: 10.1002/cmmi.1579.
[31] M. Hu, *J. Pharm. Sci.* **1993**, *82*, 829.

Supporting Information

Additional supporting information may be found in the online version of this article at the publisher's web-site.